LETTER

Tuning the Si(100) surface by Pb to yield high-Curie-temperature $Si_{1-x}Mn_x$ with MBE: A first-principles study

To cite this article: Jin Li and Lixin Zhang 2017 *EPL* **120** 47001

View the article online for updates and enhancements.

Tuning the Si(100) surface by Pb to yield high-Curie-temperature Si$_{1-x}$Mn$_x$ with MBE: A first-principles study

Jin Li[1,2] and Lixin Zhang[2(a)]

[1] *School of Material Science and Engineering, Hainan University - Hainan 570228, PRC*
[2] *School of Physics, Nankai University - Tianjin 300071, PRC*

Abstract – A high solubility and site preference for Mn doping in Si are the two keys for realizing high-Curie-temperature ferromagnetism in Si$_{1-x}$Mn$_x$. First-principles calculations reveal that both the substitutional and interstitial Mn are more favored on the Si surface than in bulk, and the substitutional Mn is more favored than the interstitial one on the reconstructed clean Si(100) surface. However, during molecular beam epitaxy, the surface is prone to further reconstructions due to the continuous deposition of feeding species. Neither substitutional nor interstitial Mn is favored, similar to that in Si bulk. Deposition of submonolayer of Pb onto the surface can restore the electronic structure of the clean surface and the favorability of the substitutional Mn, enhancing the Mn incorporation into Si significantly.

Introduction. – The discovery of ferromagnetism in transition-metal–doped semiconductors has triggered tremendous studies on the mechanism of the ferromagnetic ordering as well as on their potential applications in spintronics [1–9]. The transition metal Mn, which is expected to have the largest magnetic moment in the doped semiconductors, is generally used as the dopant. The ferromagnetic doped semiconductors are usually called diluted magnetic semiconductors (DMSs). One of the key properties of these DMSs is the Curie temperature of the ferromagnetic transition, of which the currently obtained highest value is ∼180 K for Ga$_{1-x}$AsMn$_x$ [10–12], much lower than the room temperature that is highly required by the modern electronics. Thus, to increase the Curie temperature to room temperature or above in DMSs is the central task of the related research [13,14].

Given the technological prevalence of Si, DMS based on Si is mostly interested. A relatively high Curie temperature is predicted for Mn-doped Si by mean-field theory [15,16]. However, due to the high formation energies of the Mn dopants in Si, the solubility of Mn is very low [17–19]. In experiments, Mn-ion implantation [16] and Mn δ-doping in molecular beam epitaxy (MBE) [20,21] are always employed. In Mn-ion implantation, the permanent damage to the Si lattice is harmful to the performance of the DMS. In Mn δ-doping, although the growth temperature of the material is lowered and the dynamics of the Mn atoms is limited, the resulted thin films often suffer the problem of phase separation into various SiMn phases on the surface. DMS with high Curie temperature based on Si is not reported conclusively so far.

Other than the solubility, the preferred occupation sites of the Mn dopants in Si are also very important to the strength of the exchange interactions between the Mn magnetic moments and to the Curie temperature. Thus to control the occupation site of Mn is another key to realize the expected room temperature ferromagnetism in Si.

As is well known, on the surfaces, due to the geometry change and the reconstruction of the surfaces, the favorability of an impurity or a defect can change dramatically with respect to that in the bulk [22–25]. So, during MBE, we can take advantage of the rich surface reconstructions of the semiconductors. We can tune the structure of the semiconductor surfaces, *e.g.*, by deposition of various alien atoms. From these reconstructions, we can possibly find many surfaces that may favor more the formation of Mn impurity than that in the bulk. With some unique elements or under some special conditions, we may even find

(a)E-mail: `lxzhang@nankai.edu.cn`

surfaces on which the substitutional Mn can be more favored than the interstitial one. With further epitaxy of the semiconductors, although some of the formed substitutional Mn may become interstitials through thermal diffusions, a large part of the substitutionals can be kept in the original configuration as on the surface due to the large barriers for the Mn diffusions from substitutional sites to nearby interstitial ones [24].

In this paper, taking the Mn doping through the Si(100) surface in MBE as a prototype system, we show a successful example of doping trend reversal by tuning the surface structure. We study the various reconstructions of the Si(100) surface and the competition between the formation of substitutional and interstitial Mn on these surfaces. It is revealed that on the clean surface with the popular 2×1 reconstruction, not only the formation energies of the Mn impurities are much lowered than in the bulk, but also and more interestingly, the formation of the substitutionals is more favored than the interstitials, contrasting to that in the bulk. However, during MBE, such a reconstruction is prone to further reconstructions due to the continuous deposition of feeding species. Neither interstitial nor substitutional Mn is more favored. To grow high-Curie-temperature Si-based DMS, the key is to restore the unique electronic structure of the 2×1 reconstruction of the clean surface. By studying the effect of Pb on the surface, we find that the Pb-induced reconstruction resembles electronically the clean surface and can favor the substitutional Mn doping again, given that the Pb atoms can exclude other alien atoms on the surface. Thus, using proper surfactants could be an efficient way to enhance the substitutional Mn doping in Si for high-Curie-temperature DMS.

Methods. – The calculations are performed using the Vienna *ab initio* simulation package (VASP) [26] based on the density-functional theory. The cutoff energy for plane-wave expansion is 300 eV. We use the projector augmented-wave (PAW) method and the GGA exchange-correlation functional [27]. The Si(100) surface is modeled by a slab with a $4\sqrt{2} \times 4\sqrt{2}$ surface cell, containing 12 layers of Si atoms, of which the bottom layer is passivated by H atoms. The thickness of the vacuum layer is more than 10 Å and the M-P k-point mesh is $2 \times 2 \times 1$. The calculated equilibrium lattice constant for bulk Si is 5.46 Å, in good agreement with experimental value of 5.43 Å [28].

For various surfaces, their energies are calculated by

$$E_{\rm s} = E_{\rm d} - E_{\rm clean} - m \cdot \mu_{\rm Pb} - n \cdot \mu_{\rm H}, \qquad (1)$$

where $E_{\rm d}$ is the total energy of the H- or Pb-decorated surface and $E_{\rm clean}$ the clean surface, m and n are the number of Pb and H atoms on the surface. The formation energy of a substitutional Mn at the Si(100) surface is given by

$$E_{\rm f}^{(\rm s)} = E_{\rm tot} - E_{\rm ref} + \mu_{\rm Si} + l \cdot \mu_{\rm H} - \mu_{\rm Mn}, \qquad (2)$$

where $E_{\rm tot}$ is the total energy of the Mn substituted surface, $E_{\rm ref}$ is the total energy of the corresponding Si(100)

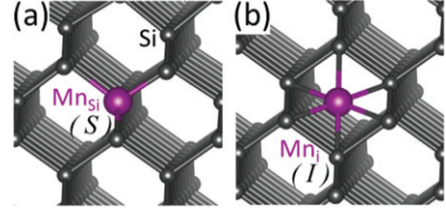Fig. 1: (Color online) The perspective views of (a) a $Mn_{\rm Si}$ and (b) a $Mn_{\rm i}$ in bulk Si. All of the substitutional sites (designated by S) for Mn are identical in bulk Si. All of the interstitial sites (designated by I) are identical as well.

surface (acting as the reference) without Mn, and l is the number of H atoms simultaneously removed from the reference structure. The symbols $\mu_{\rm Si}$, $\mu_{\rm H}$, $\mu_{\rm Pb}$ and $\mu_{\rm Mn}$ are the chemical potentials of Si, H, Pb and Mn. The calculated chemical potentials of Si, Pb, and Mn in their bulk phases are -5.43 eV, -3.54 eV, and -8.89 eV, respectively. The calculated chemical potential of H in gas H_2 is -3.38 eV. For an interstitial Mn, the formation energy is simply given by

$$E_{\rm f}^{(\rm i)} = E_{\rm tot} - E_{\rm ref} - \mu_{\rm Mn}. \qquad (3)$$

Results and discussion. – In fig. 1, the configurations of a substitutional Mn ($Mn_{\rm Si}$) and an interstitial Mn ($Mn_{\rm i}$) in bulk Si are shown. Their formation energies are calculated and listed in the bottom of table 1. If we use the bulk energies of Si and Mn for $\mu_{\rm Si}$ and $\mu_{\rm Mn}$, the formation energies of the two types of Mn are 2.60 eV and 2.15 eV, respectively. The two relative large positive values indicate that the formation of neither Mn impurity is favored in bulk Si. It can be further seen that the $Mn_{\rm Si}$ is more unfavored by 0.45 eV than the $Mn_{\rm i}$. The relative large formation energy and the less favorability of the $Mn_{\rm Si}$ in Si are the two obstacles for realizing Mn-doped DMS in Si.

We should note that part of the calculations in this study has already been done in many previous studies, *i.e.*, ref. [25] and reference therein. Our results are agreeable with them. The reason we show them in the paper repeatedly is twofold. One is for consistency and the conveniences of the readers, one is for the different perspectives of the calculated data.

In fig. 2(a), the atomic structure of the clean Si(100) surface with the popular 2×1 reconstruction is shown. This structure is energetically the most favored and is characterized by the dimer rows composed of alternating buckled dimers. Unlike in bulk, at the top surface layer, there are three types of substitutional sites, as designated by S_1, S_2, and S_3, and two types of interstitial sites, as designated by I_1 and I_2, respectively. The two Si atoms at the S_1 and S_2 sites form the so-called buckled dimer. For $Mn_{\rm i}$, the I_2 site is always more favored than the I_1 site, thus in table 1, the formation energies for the $Mn_{\rm i}$ are all for I_2 sites. For $Mn_{\rm Si}$, the formation energies at the three surface sites are contrasting. At S_2 site, the formation energy

Table 1: The surface energies of various Si(100) surfaces, and the formation energies of the most favored Mn_{Si} and Mn_i at these surfaces.

Surfaces	Surface energy (per $4\sqrt{2} \times 4\sqrt{2}$ unit cells)	Substitutional Mn Mn_{Si}		Interstitial Mn Mn_i
		Formation energy $E_f^{(s)}$	Structural configuration	Formation energy $E_f^{(i)}$
Clean surface	$0^{(a)}$	$-1.39 - \mu_{Mn} + \mu_{Si} \ (2.07)^{(b)}$	S_1	$-7.98 - \mu_{Mn} \ \mathbf{(0.91)}^{(b)}$
	$(0)^{(b)}$	$-3.27 - \mu_{Mn} + \mu_{Si} \ \mathbf{(0.19)}$	S_2	
		$-1.62 - \mu_{Mn} + \mu_{Si} \ (1.84)$	S_3	
H-fully decorated	$-138.90 - 32\mu_H$ (-30.84)	$0.08 - \mu_{Mn} + \mu_{Si} \ (3.54)$	S_1	$-6.36 - \mu_{Mn} \ (2.53)$
		$3.96 - \mu_{Mn} + \mu_{Si} + \mu_H$ (4.05)	S_1, with the H on S_1 removed	
		$7.39 - \mu_{Mn} + \mu_{Si} + 2\mu_H \ (4.10)$	S_1, with two H's on the dimer removed	
		$-0.41 - \mu_{Mn} + \mu_{Si} \ (3.05)$	S_3	
Pb-decorated	$25.68 - 16\mu_{Pb} + 16\mu_{Si}$ (-4.58)	$-3.36 - \mu_{Mn} + \mu_{Si} \ \mathbf{(0.10)}$	S_2	$-7.9 - \mu_{Mn} \ (0.98)$
		$-2.51 - \mu_{Mn} + \mu_{Si} \ (0.96)$	S_3	
Pb- and H-decorated	$-36.83 - 16\mu_{Pb} + 16\mu_{Si}$ $-16\mu_H$ (-13.07)	$-1.11 - \mu_{Mn} + \mu_{Si} \ (2.35)$	S_2	$-8.18 - \mu_{Mn} \ \mathbf{(0.71)}$
		$2.34 - \mu_{Mn} + \mu_{Si} + \mu_H \ (2.42)$	S_2, with the H removed	
		$-1.36 - \mu_{Mn} + \mu_{Si} \ (2.10)$	S_3	
Bulk	–	$-0.86 - \mu_{Mn} + \mu_{Si} \ (2.60)$	–	$-6.74 - \mu_{Mn} \ (2.15)$

[a] The values of the energies are in units of eV and the energy of the reconstructed clean surface is set to 0.
[b] The values in the brackets are the corresponding energies with $\mu_{Si} = -5.43\,eV$, $\mu_H = -3.38\,eV$, and $\mu_{Pb} = -3.54\,eV$.

(0.19 eV) is the lowest. Two points can be drawn from the data in table 1 for the clean surface. One is that the formation energies of both Mn impurities at the surface can be much lowered than that in the bulk. The other is that the formation energy of a Mn_{Si} (the lowest is 0.19 eV), contrasting to that in the bulk, can be lower than a Mn_i (the lowest is 0.91 eV). The conclusion is that, with this surface structure dominating, the solubility of Mn can be greatly enhanced, and the Mn dopant prefers to occupy the substitutional site. With the epitaxy going on, the substitutional doping will dominate in the Mn-doped Si which is highly required for DMS.

The electronic origin is obvious for this result. As shown in fig. 2(b), in the buckled Si dimer, a simple electron-counting rule [29] requires that the Si at the S_1 site has a fully filled dangling bond and the Si at the S_2 site has a fully empty dangling bond. With Mn (usually takes the 2+ charge state) substituting the Si (four valence electrons) at the S_2 site, the system can still satisfy the electron-counting rule by just emptying the dangling bond at the S_1 site which usually has a higher energy level (the Si atom will relax downward). Thus the structure with the substituting Mn at the S_2 site is very stable. The Mn atom can also substitute the Si at S_1 site and the remained Si at the S_2 site relaxes upward which results in an identical
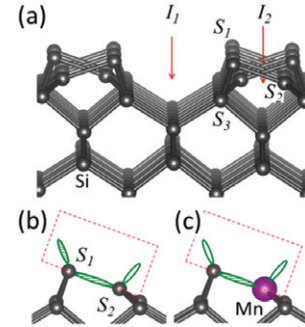

Fig. 2: (Color online) (a) The atomic structure of the clean Si(100) surface. The buckled dimers alternate along the dimer row direction. Different substitutional sites (S_1, S_2, and S_3) and interstitial sites (I_1, I_2) at the surface are designated. Schematics for the chemical bonds (b) in a Si dimer and (c) in a Si-Mn pair with a Mn_{Si} at the S_2 site. The filled and empty ovals stand for the filled and empty chemical (dangling) bonds.

structure. On the other hand, the two electrons from an interstitial Mn must fill the dangling bond at the S_2 site (originally empty) which is even higher in energy. Thus, it is the unique reconstruction of the 2×1 surface that makes the Mn_{Si} more favored than the Mn_i at the Si(100) clean surface, and both are more favored than in the bulk.
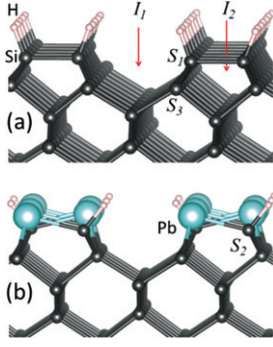
Fig. 3: (Color online) (a) The atomic structure of the H- fully decorated Si(100) surface. The large relaxations on the clean surface are totally reduced. The S_1 site and the S_2 site are identical, thus the S_2 site is not designated again. (b) The atomic structure of the Pb and H- decorated Si(100) surface.
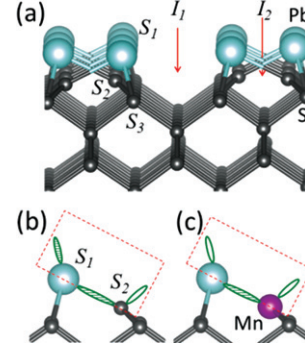

Fig. 4: (Color online) (a) The atomic structure of the Pb-induced Si(100) with 1/2 monolayer of Pb on the surface. Note that the Si at the S_2 site has similar configuration to that in fig. 2. Schematics for the chemical bonds in (b) a Pb-Si pair and in (c) a Pb-Mn pair after the Mn substitution on the surface. The filled and empty ovals stand for the filled and empty chemical (dangling) bonds.

It seems that the above results contradict the experiments. From MBE experiments on the Si(100) surface, it is well known that the Mn-doped DMS is very hard to realize. This indicates that the Mn_{Si} could not be favored at the growth front surface, or to say that the buckled dimer row structure of the clean surface may not dominate during the MBE process.

We know that the buckled dimer row structure is usually obtained in high vacuum, and after very demanding surface cleaning processes [30]. In MBE however, the above conditions for the surface could not be satisfied due to the continuous feeding of the source species. With feeding species on the Si(100) surface, the buckled dimer structure is no longer stable and further reconstructions will take place. We can use the difference between the relaxations of the S_1 and S_2 sites (ΔR_{S12}) as a measure of the further reconstruction of the surface. Generally speaking, the feeding species on the clean surface will reduce the value of ΔR_{S12}.

Here, we take hydrogen as a representative feeding atom. In fig. 3, the reduced surface under 1 monolayer of hydrogen is shown. It can be seen that the distinct surface sites S_1 and S_2 in fig. 2 become identical at the hydrogen fully covered surface, i.e., $\Delta R_{S12} = 0$. We calculated the energy of this surface as well as the formation energies of Mn_{Si} and Mn_i. The results are shown in table 1, too. We see that firstly, the H-decorated surface is more stable than the clean surface. Under hydrogen-rich condition, the surface energy is $\sim 1\,eV$ ($-30.84/4\sqrt{2}/4\sqrt{2}$) lower per unit cell than that of the buckled dimer structure. Secondly, both of the formation energies of the Mn_{Si} and Mn_i (the lowest values are $3.05\,eV$ and $2.53\,eV$, respectively) are increased rather than decreased with respect to the counterpart bulk values. There are no sites at the surface for Mn_{Si} to be more favorable than the Mn_i. This indicates that neither Mn_{Si} nor Mn_i is favored on such a surface. This result seems more consistent with the experiments which showed that phase separations on the surface dominate [31].

It is natural to wonder if there are atoms that function distinctly from the hydrogen atoms on the surface. With these atoms the surface can keep the ΔR_{S12} value of the clean surface as much as possible. Inspired by ref. [20], we turn to Pb which is in the same group as Si but with much larger radius. It also has four outermost electrons but divided into two subgroups. On the Si(100) surface, Pb will float on the surface and act as a surfactant [32]. Furthermore, Pb can replace half of the surface Si atoms and turn the buckled Si dimer row structure into a buckled Pb-Si pair row structure. In fig. 4 the most stable Pb-induced surface reconstruction is shown. Because the Pb atoms are chemically bonded to the Si lattice, being less active than Si, and much heavier than other feeding atoms, they will remain on the surface as a stable surfactant during the MBE process. This means that the Pb-Si pair structure, unlike the Si buckled dimer structure of the clean surface, can be more robust against the feeding species. In the Pb-induced reconstruction, the Si atom at S_2 site is chemically similar to that on the clean surface. It is expected that the substitutional Mn can be favored again.

The surface energy and the formation energies for Mn dopants are calculated and the results are listed in table 1, too. We can see that the energy of the Pb-decorated surface ($-4.58\,eV$ per 32 unit cells) is lower than that of the clean surface under the Pb-rich condition. For the substitutional Mn and the interstitial Mn at the surface, the most favorable formation energies ($0.10\,eV$ and $0.98\,eV$) both are lower than their bulk counterparts. More importantly, the substitutional Mn could be more favorable than the interstitial one similar to that on the clean surface. The electronic origin is also similar to that on the clean surface as shown in fig. 4. After the Mn substituting at the S_2 site, the structure can satisfy the electron-counting rule by emptying the dangling bond on the S_1 site as shown in fig. 4(c).

The Pb-decorated surface is not immune to H. As shown in fig. 3(b), the H atoms will bind to the Si atoms at S_2 site on the surface. As shown in table 1, the surface energy can be further decreased (to -13.07 eV per 32 unit cells) with respect to the Pb-decorated surface. At this time, the substitutional Mn is no longer favored. At the S_2 site, the formation energy of a substitutional Mn is close to that in the bulk again. For interstitial Mn, on the other hand, the formation energy is much lower than that in the bulk. This indicates that with Pb and H on the surface, the interstitial Mn is the most favored. This can also be explained by a simple electron counting of the system. In the interstitial case, the two electrons on Mn are nominally donated to the Pb atom where the empty dangling bond can be just filled (lower than the conduction band).

There is one more issue to be clarified. On the Pb- and H-decorated surface, if Mn substitutes the Si at the S_2 site with the H atom simultaneously removed, the configuration is similar to the one on the Pb-decorated surface which means that locally the electronic environments for Mn atoms should be similar, too. In the later case the formation energy of the substitutional Mn is very low, as low as 0.10 eV. But, in the former case, it is 2.42 eV (see table 1). Why are the formation energies of the two cases different so much? This is because the energies of the respective reference structures in the formation energy calculations are different. In the former case, it is the Pb- and H-decorated surface whose energy is lower. In the later case, it is the Pb-decorated surface whose energy is higher. This tells us that to maintain a relatively high energy of the surface is the key for the favored substitutional Mn doping.

There is another important issue with the incorporation of the transition metal atoms on the growth surface. That is the interaction between these atoms when their density is high on the surface. We can calculate the paring energy as the method discussed in a recent review [2]. Our calculations show that on the clean Si (100) surface, interstitial Mn atoms expel each other and substitutional ones attract. Two Mn atoms located at the nearest-neighbour Si sites on two consecutive layers along the (100) direction have the lowest pairing energy of -0.79 eV, which indicates a strong clustering tendency for the incorporated substitutional Mn atoms on the Si (100) surface. On a Pb-decorated surface, the results are similar. In these cases, there is also no preference for the two Mn atoms to bind either ferromagnetically or antiferromagnetically, contrasting to that in e.g., III-V semiconductors [33]. This poses some extra challenges to the control of growth conditions. In theoretical side, the entropy term and diffusion kinetics should be further studied to shed more light on this issue.

Conclusion. – In conclusion, our study shows that during the Mn incorporation into Si in the MBE process, the surface dynamical structures play the key roles. The clean Si (100) surface usually assumes a buckled dimer structure which is favorable for Mn substitutional doping. Unfortunately during MBE, this structure is no longer dominating. Further calculations show that the submonolayer of Pb on the surface not only can restore the unique electronic structure of the buckled dimers, but also can make the induced reconstruction live longer than the buckled dimer structure of the clean surface. H is detrimental to the substitutional doping of Mn and should be rigorously excluded during Si MBE. Our work further approves that surface science study is important to resolve the many difficulties encountered in the growth of various functional materials.

$$* * *$$

REFERENCES

[1] Ohno H., *Science*, **281** (1998) 951.
[2] Dietl T., Sato K., Fukushima T., Bonanni A., Jamet M., Barski A., Kuroda S., Tanaka M., Hai P. N. and Katayama-Yoshida H., *Rev. Mod. Phys.*, **87** (2015) 1311.
[3] Sato K., Bergqvist L., Kudrnovsky J., Dederichs P. H., Eriksson O., Turek I., Sanyal B., Bouzerar G., Katayama-Yoshida H., Dinh V. A., Fukushima T., Kizaki H. and Zeller R., *Rev. Mod. Phys.*, **82** (2010) 1633.
[4] Fukumura T., Toyosaki H. and Yamada Y., *Semicond. Sci. Technol.*, **20** (2005) S103.
[5] Dietl T. and Ohno H., *Rev. Mod. Phys.*, **86** (2014) 187.
[6] Patzke G. R., Zhou Y., Kontic R. and Conrad F., *Angew. Chem., Int. Ed.*, **50** (2011) 826.
[7] Feng Y. P., Shen L., Yang M., Wang A., Zeng M., Wu Q., Chintalapati S. and Chang C.-R., *WIREs Comput. Mol. Sci.* (2017) e1313.
[8] Wu M. W., Jiang J. H. and Weng M. Q., *Phys. Rep.*, **493** (2010) 61.
[9] Žutić I., Fabian J. and Das Sarma S., *Rev. Mod. Phys.*, **76** (2004) 323.
[10] Edmonds K. W., Wang K. Y., Campion R. P., Neumann A. C., Farley N. R. S., Gallagher B. L. and Foxon C. T., *Appl. Phys. Lett.*, **81** (2002) 4991.
[11] Wang M., Campion R. P., Rushforth A. W., Edmonds K. W., Foxon C. T. and Gallagher B. L., *Appl. Phys. Lett.*, **93** (2008) 132103.
[12] Olejník K., Owen M. H. S., Novák V., Mašek J., Irvine A. C., Wunderlich J. and Jungwirth T., *Phys. Rev. B*, **78** (2008) 054403.
[13] Bergqvist L., Eriksson O., Kudrnovský J., Drchal V., Korzhavyi P. and Turek I., *Phys. Rev. Lett.*, **93** (2004) 137202.
[14] Reed M. L., El-Masry N. A., Stadelmaier H. H., Ritums M. K., Reed M. J., Parker C. A., Roberts J. C. and Bedair S. M., *Appl. Phys. Lett.*, **79** (2001) 3473.

[15] DIETL T., *Semicond. Sci. Technol.*, **17** (2002) 377.

[16] BOLDUC M., AWO-AFFOUDA C., STOLLENWERK A., HUANG M. B., RAMOS F. G., AGNELLO G. and LABELLA V. P., *Phys. Rev. B*, **71** (2005) 033302.

[17] BERNARDINI F., PICOZZI S. and CONTINENZA A., *Appl. Phys. Lett.*, **84** (2004) 2289.

[18] MUKHOPADHYAY S. and HARRISON N. M., *J. Magn. & Magn. Mater.*, **324** (2012) 3748.

[19] STROPPA A., PICOZZI S., CONTINENZA A. and FREEMAN A. J., *Phys. Rev. B*, **68** (2003) 155203.

[20] KAHWAJI S., GORDON R. A., CROZIER E. D., ROORDA S., ROBERTSON M. D., ZHU J. and MONCHESKY T. L., *Phys. Rev. B*, **88** (2013) 174419.

[21] ZHANG Y., JIANG Q., SMITH D. J. and DRUCKER J., *J. Appl. Phys.*, **98** (2005) 033512.

[22] ERWIN S. C., ZU L., HAFTEL M. I., EFROS A. L., KENNEDY T. A. and NORRIS D. J., *Nature*, **436** (2005) 91.

[23] OHTAKE A., HAGIWARA A. and NAKAMURA J., *Phys. Rev. B*, **87** (2013) 165301.

[24] ZHU W., WEITERING H. H., WANG E. G., KAXIRAS E. and ZHANG Z., *Phys. Rev. Lett.*, **93** (2004) 126102.

[25] DA SILVA A. J. R. and FAZZIO A., *Phys. Rev. B*, **70** (2004) 193205.

[26] KRESSE G. and HAFNER J., *Phys. Rev. B*, **47** (1993) R558; **49** (1994) 14251.

[27] PERDEW J. P., BURKE K. and ERNZERHOF M., *Phys. Rev. Lett.*, **77** (1996) 3865.

[28] WYCKOFF R. W. G., *Crystal Structures*, Vol. **1**, second editon (Wiley) 1963, pp. 26–27.

[29] ZHANG L., WANG E. G., XUE Q. K., ZHANG S. B. and ZHANG Z., *Phys. Rev. Lett.*, **97** (2006) 126103.

[30] KRAUSE M. R., STOLLENWERK A. J., REED J. and LABELLA V. P., *Phys. Rev. B*, **75** (2007) 205326.

[31] MEN'SHOV V. N., TUGUSHEV V. V., CAPRARA S. and CHULKOV E. V., *Phys. Rev. B*, **83** (2011) 035201.

[32] XIAO Q. F., KAHWAJI S., MONCHESKY T. L., GORDON R. A. and CROZIER E. D., *J. Phys.: Conf. Ser.*, **190** (2009) 012101.

[33] GONZALEZ SZWACKI N., MAJEWSKI J. A. and DIETL T., *Phys. Rev. B*, **83** (2011) 184417.